J. theor. Biol. (1999) **198,** 445–459
Article No. jtbi.1999.0924, available online at http://www.idealibrary.com on IDEAL

Chaos and Birhythmicity in a Model for Circadian Oscillations of the PER and TIM Proteins in *Drosophila*

JEAN-CHRISTOPHE LELOUP AND ALBERT GOLDBETER*

Unité de Chronobiologie Théorique, Faculté des Sciences, Université Libre de Bruxelles, Campus Plaine, C.P. 231, *B*-1050 *Brussels, Belgium*

(*Received on* 13 *July* 1998, *Accepted in revised form on* 12 *February* 1999)

In *Drosophila*, circadian oscillations in the levels of two proteins, PER and TIM, result from the negative feedback exerted by a PER–TIM complex on the expression of the *per* and *tim* genes which code for these two proteins. On the basis of these experimental observations, we have recently proposed a theoretical model for circadian oscillations of the PER and TIM proteins in *Drosophila*. Here we show that for constant environmental conditions this model is capable of generating autonomous chaotic oscillations. For other parameter values, the model can also display birhythmicity, i.e. the coexistence between two stable regimes of limit cycle oscillations. We analyse the occurrence of chaos and birhythmicity by means of bifurcation diagrams and locate the different domains of complex oscillatory behavior in parameter space. The relative smallness of these domains raises doubts as to the possible physiological significance of chaos and birhythmicity in regard to circadian rhythm generation. Beyond the particular context of circadian rhythms we discuss the results in the light of other mechanisms underlying chaos and birhythmicity in regulated biological systems.

1. Introduction

Circadian oscillations, of about 24 hr period, occur in nearly all living organisms, and are among the most conspicuous biological rhythms. Important insights into the molecular mechanisms underlying circadian rhythm generation have been gained from the study of organisms such as *Drosophila* (Konopka & Benzer, 1971; Hall & Rosbash, 1987; Baylies *et al*., 1993; Hall, 1995; Rosbash, 1995) and *Neurospora* (Dunlap, 1996; Crosthwaite *et al*., 1997). In *Drosophila*, circadian oscillations in the levels of two proteins, PER and TIM, result from the negative feedback exerted by a PER–TIM complex on the expression of the *per* and *tim* genes which code for the two proteins (Hunter-Ensor *et al*., 1996; Lee *et al*., 1996; Myers *et al*., 1996; Zeng *et al*., 1996). The *per* and *tim* genes have recently been found in mammals (Shearman *et al*., 1997; Tei *et al*., 1997; Koike *et al*., 1998; Zylka *et al*., 1998), including man. This suggests that the circadian clock mechanism might be conserved at least partly, if not entirely, from *Drosophila* to mammals.

Based on these experimental observations, we have recently proposed a theoretical model for circadian oscillations of the PER and TIM proteins in *Drosophila* (Leloup & Goldbeter, 1998), which extends a previous version based on regulation by PER alone (Goldbeter, 1995, 1996). The extended model accounts for a number of experimental observations such as the

*Author to whom correspondence should be addressed. E-mail: agoldbet@ulb.ac.be

0022–5193/99/011445 + 15 $30.00/0

generation of circadian oscillations in constant darkness, phase shifting by light pulses, and entrainment by a light–dark cycle of appropriate period (Leloup & Goldbeter, 1998). That negative feedback on gene expression may give rise to oscillations was first pointed out by Goodwin (1965) who proposed a model which was later used to study properties of circadian rhythms (Ruoff *et al*., 1996).

Somewhat surprisingly we have found that the model incorporating the formation of a complex between the PER and TIM proteins (Leloup & Goldbeter, 1998) not only can account for regular oscillations of circadian period in constant environmental conditions, but also may give rise in such conditions to more complex oscillatory phenomena including chaos and birhythmicity, i.e. the coexistence of two stable regimes of limit cycle oscillations (Decroly & Goldbeter, 1982; Goldbeter, 1996). The purpose of the present article is to determine the conditions in which such modes of complex nonlinear dynamics arise in the model for circadian oscillations of the PER and TIM proteins in *Drosophila*.

In Section 2 we present the model for circadian oscillations in PER and TIM, as well as the system of 10 kinetic equations which govern its time evolution. Evidence for chaotic behavior is presented in Section 3. We show in Section 4 that the model is also capable of birhythmicity. The domains in which these various modes of complex oscillatory phenomena occur in parameter space, as well as the domain of simple periodic oscillations (which remain the most common mode of oscillatory behavior), are determined in Section 5. In the last section we discuss the significance of the results in regard to circadian rhythm generation and consider, in a more general context, how they bear on the origin of chaos and birhythmicity in regulated biological systems.

2. Model for *Drosophila* Circadian Rhythms Involving the Formation of a Complex Between PER and TIM

The model, schematized in Fig. 1, relies on the following assumptions (see Fig. 1 and its legend for a definition of the parameters): *per* messenger RNA (mRNA), the cytosolic concentration of which is denoted by M_P, is synthesized in the nucleus and transfers to the cytosol, where it is degraded; the rate of synthesis of PER is proportional to M_P. To take into account the fact that PER is multiply phosphorylated (Edery *et al*., 1994), and to keep the model as simple as possible (the precise number of phosphorylated residues is still unknown), only three states of the protein are considered: unphosphorylated (P_0), mono- (P_1) and bisphosphorylated (P_2). The model could readily be extended to include a larger number of phosphorylated residues; we checked that such an extension would unnecessarily complicate the model without altering significantly its dynamic behavior. The kinase that phosphorylates PER has recently been identified as being the product of the gene *double-time* (*dbt*) (Kloss *et al*., 1998; Price *et al*., 1998). The maximum rate of that kinase in the model is denoted by V_{1P} and V_{3P} for the first and second phosphorylations of PER (see Fig. 1).

To take into account the role played by the formation of a complex between the PER and TIM proteins, we consider a sequence of steps for TIM similar to the one outlined above for PER. Thus we assume that *tim* mRNA, whose cytosolic concentration is denoted by M_T, is synthesized in the nucleus and transfers to the cytosol, where it is degraded; the rate of TIM synthesis is proportional to M_T. For reasons of symmetry with PER, we further assume that TIM is phosphorylated in a reversible manner, into the forms T_1 and T_2; such covalent modifications have recently been observed (Zeng *et al*., 1996). The effect of light–dark (LD) cycles on the dynamics of the PER–TIM system can readily be incorporated into the model (see Fig. 1) by noticing that TIM degradation is controlled by light (Hunter-Ensor *et al*., 1996; Lee *et al*., 1996; Myers *et al*., 1996; Zeng *et al*., 1996). Thus, parameter v_{dT}, which measures the maximum rate of TIM degradation, varies periodically in LD cycles (Leloup & Goldbeter, 1998).

The role of PER and TIM phosphorylation is still unclear. Here we assume that the fully phosphorylated form (P_2) is marked both for degradation — this hypothesis holds with experimental observations (Edery *et al*., 1994; Price

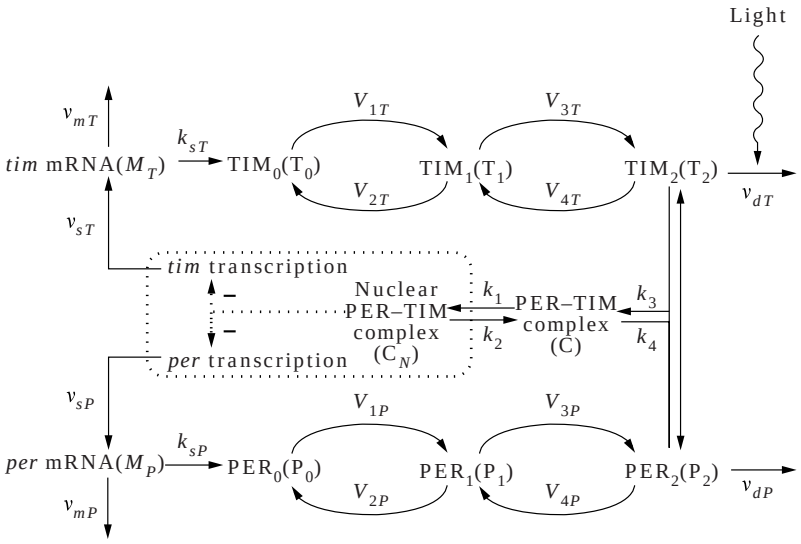

FIG. 1. Scheme of the model for circadian oscillations in *Drosophila* involving negative regulation of gene expression by a complex between PER and TIM (Leloup & Goldbeter, 1998). *per* (M_P) and *tim* (M_T) mRNAs are synthesized in the nucleus and transferred into the cytosol, where they accumulate at the maximum rates v_{sP} and v_{sT}, respectively; there they are degraded enzymatically at the maximum rates v_{mP} and v_{mT}, with the Michaelis constants K_{mP} and K_{mT}. The rates of synthesis of the PER and TIM proteins, respectively proportional to M_P and M_T, are characterized by the apparent first-order rate constant k_{sP} and k_{sT}. Parameters V_{iP}, V_{iT} and K_{iP}, K_{iT} ($i = 1, \ldots 4$) denote the maximum rate and Michaelis constant of the kinase(s) and phosphatase(s) involved in the reversible phosphorylation of P_0 (T_0) into P_1 (T_1) and P_1 (T_1) into P_2 (T_2), respectively. The fully phosphorylated forms (P_2 and T_2) are degraded by enzymes of maximum rate v_{dP}, v_{dT} and Michaelis constants K_{dP}, K_{dT}, and reversibly form a complex C (with the forward and reverse rate constants k_3, k_4) which is transported into the nucleus at a rate characterized by the apparent first-order rate constant k_1. Transport of the nuclear form of the PER–TIM complex (C_N) into the cytosol is characterized by the apparent first-order rate constant k_2. The negative feedback exerted by the nuclear PER–TIM complex on *per* and *tim* transcription is described by an equation of the Hill type [see first term in eqns (1a) and (1e)], in which n denotes the degree of cooperativity, and K_{IP} and K_{IT} the threshold constants for repression.

et al., 1998) — and for the reversible formation of a complex C with the fully modified form T_2 of TIM, which is similarly marked for degradation. In the model, phosphorylation of PER and TIM favours sustained oscillations but is not required for their occurrence (Leloup & Goldbeter, 1998). The PER–TIM complex (C_N) is transported into the nucleus where it exerts a negative feedback on the production of *per* and *tim* mRNAs. This negative feedback is described by an equation of the Hill type. For simplicity, we consider that C_N behaves directly as a repressor; indirect repression through interaction of C_N with the products of the genes *Jrk* and *cyc* (also known, respectively, as *dclock* and *dbmal*1) which dimerize to promote *per* and *tim* expression (Allada *et al*., 1998; Darlington *et al*., 1998; Rutila *et al*., 1998) would not significantly alter the results. Finally, all equations contain a linear degradation term, characterized by the rate constant k_d (k_{dC} and k_{dN} for the cytoplasmic and nuclear forms of the PER–TIM complex, respectively); this term, of small magnitude, is not required for oscillations but serves to ensure that a steady state always exists even when specific degradation processes are inhibited. Since the non-specific degradation rate constants are relatively small, and only serve to prevent any unbounded accumulation of the variables, we verified that similar results are obtained when taking different values for such constants, for each of the variables of the model.

2.1. KINETIC EQUATIONS

Denoting the concentration of species X_i by X_i, the time evolution of the 10-variable model is governed by the following kinetic equations, in which all parameters and concentrations are defined with respect to the total cell volume (Leloup & Goldbeter, 1998):

$$\frac{dM_P}{dt} = v_{sP}\frac{K_{IP}^n}{K_{IP}^n + C_N^n} - v_{mP}\frac{M_P}{K_{mP} + M_P} - k_d M_P \qquad (1a)$$

$$\frac{dP_0}{dt} = k_{sP}M_P - V_{1P}\frac{P_0}{K_{1P}+P_0} + V_{2P}\frac{P_1}{K_{2P}+P_1} - k_dP_0 \quad (1b)$$

$$\frac{dP_1}{dt} = V_{1P}\frac{P_0}{K_{1P}+P_0} - V_{2P}\frac{P_1}{K_{2P}+P_1} - V_{3P}\frac{P_1}{K_{3P}+P_1} + V_{4P}\frac{P_2}{K_{4P}+P_2} - k_dP_1 \quad (1c)$$

$$\frac{dP_2}{dt} = V_3P\frac{P_1}{K_{3P}+P_1} - V_{4P}\frac{P_2}{K_{4P}+P_2} - k_3P_2T_2 + k_4C - v_{dP}\frac{P_2}{K_{dP}+P_2} - k_dP_2 \quad (1d)$$

$$\frac{dM_T}{dt} = v_{sT}\frac{K_{IT}^n}{K_{IT}^n+C_N^n} - v_{mT}\frac{M_T}{K_{mT}+M_T} - k_dM_T \quad (1e)$$

$$\frac{dT_0}{dt} = k_{sT}M_T - V_{1T}\frac{T_0}{K_{1T}+T_0} + V_{2T}\frac{T_1}{K_{2T}+T_1} - k_dT_0 \quad (1f)$$

$$\frac{dT_1}{dt} = V_{1T}\frac{T_0}{K_{1T}+T_0} - V_{2T}\frac{T_1}{K_{2T}+T_1} - V_{3T}\frac{T_1}{K_{3T}+T_1} + V_{4T}\frac{T_2}{K_{4T}+T_2} - k_dT_1 \quad (1g)$$

$$\frac{dT_2}{dt} = V_{3T}\frac{T_1}{K_{3T}+T_1} - V_{4T}\frac{T_2}{K_{4T}+T_2} - k_3P_2T_2 + k_4C - v_{dT}\frac{T_2}{K_{dT}+T_2} - k_dT_2 \quad (1h)$$

$$\frac{dC}{dt} = k_3P_2T_2 - k_4C - k_1C + k_2C_N - k_{dC}C \quad (1i)$$

$$\frac{dC_N}{dt} = k_1C - k_2C_N - k_{dN}C_N. \quad (1j)$$

The total (non-conserved) quantity of PER and TIM proteins, P_t and T_t, are given by:

$$P_t = P_0 + P_1 + P_2 + C + C_N \quad (2)$$

$$T_t = T_0 + T_1 + T_2 + C + C_N. \quad (3)$$

2.2. GENERATION OF PERIODIC, CIRCADIAN OSCILLATIONS

As reported in our previous publication (Leloup & Goldbeter, 1998), the model governed by eqns (1a)–(1j) readily gives rise to sustained oscillations of the limit cycle type. These simple periodic oscillations, which correspond to circadian rhythmicity, are by far the most common mode of oscillatory behavior in parameter space (see Section 5 below). An example of such periodic oscillations is shown in Fig. 2, in conditions corresponding to constant darkness. This figure illustrates a key property of circadian rhythms, which pertains to their endogenous nature, since they can occur in a constant environment. When parameter v_{dT} varies in a square-wave manner due to the forcing by LD cycles, entrainment to the external periodicity can be observed provided that the forcing period is in an appropriate range (Leloup & Goldbeter, 1998).

We shall not return here to the occurrence of simple periodic behavior in the model, which was considered in detail in a recent pulication (Leloup & Goldbeter, 1998), and will focus instead on the occurrence of complex oscillatory phenomena including chaos and birhythmicity.

3. Chaos

Although chaos can readily originate from the periodic forcing of an oscillatory system, we shall only consider the occurrence of autonomous chaos which occurs when the system operates in constant environmental conditions, i.e. constant darkness (DD) or constant light (LL). Chaos has also been obtained in a closely related circadian model in response to periodic forcing by LD cycles (Gonze *et al.*, 1999).

The numerical integration of the kinetic equations (1a)–(1j) shows that autonomous chaos can be observed in the present model over a relatively large range of parameter values. Typical chaotic oscillations generated by the model are shown in Fig. 3, where the irregular time evolution of *per* and *tim* mRNAs (upper and middle panels, respectively) is represented, together with that of the nuclear PER–TIM complex (lower panel). For the parameter values

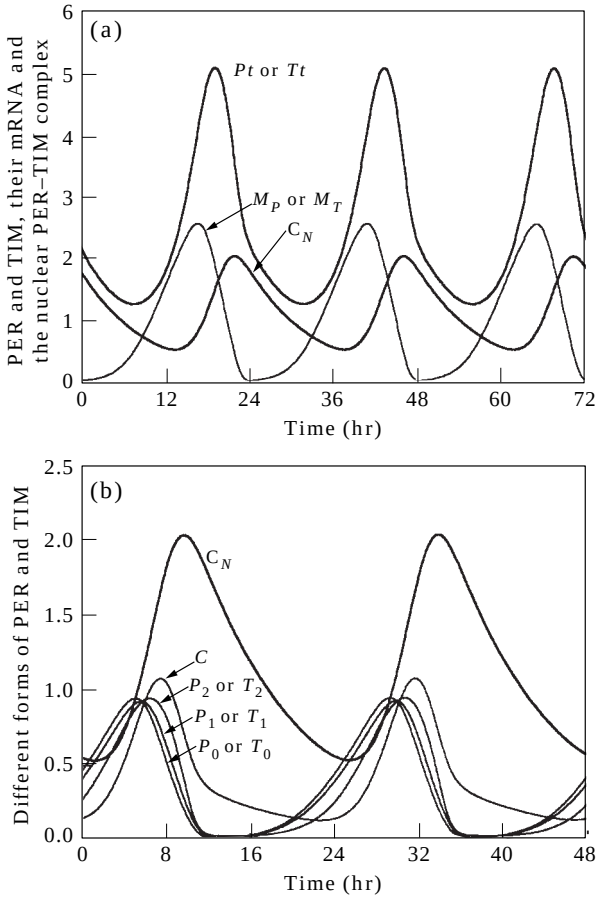

FIG. 2. Sustained oscillations generated by the model based on negative control of *per* and *tim* expression by a PER–TIM complex in *Drosophila* (Leloup & Goldbeter, 1998). Shown is the temporal variation in *per* and *tim* mRNAs (M_P and M_T) and in the total amount of PER and TIM proteins (P_t, T_t), together with the variation in nuclear PER–TIM complex (C_N). The curves are obtained by numerical integration of eqns (1a)–(1j) in conditions corresponding to constant darkness; P_t and T_t are given by eqns (2, 3). Parameter values are: $v_{sP} = v_{sT} = 1$ nM hr^{-1}, $v_{mP} = v_{mT} = 0.7$ nM hr^{-1}, $v_{dP} = v_{dT} = 2$ nM hr^{-1}, $k_{sP} = k_{sT} = 0.9$ hr^{-1}, $k_1 = 0.6$ hr^{-1}, $k_2 = 0.2$ hr^{-1}, $k_3 = 1.2$ nM^{-1} hr^{-1}, $k_4 = 0.6$ hr^{-1}, $K_{mP} = K_{mT} = 0.2$ nM, $K_{IP} = K_{IT} = 1$ nM, $K_{dP} = K_{dT} = 0.2$ nM, $K_{1P} = K_{1T} = K_{2P} = K_{2T} = K_{3P} = K_{3T} = K_{4P} = K_{4T} = 2$ nM, $V_{1P} = V_{1T} = 8$ nM hr^{-1}, $V_{2P} = V_{2T} = 1$ nM hr^{-1}, $V_{3P} = V_{3T} = 8$ nM hr^{-1}, $V_{4P} = V_{4T} = 1$ nM hr^{-1}, $k_d = k_{dC} = k_{dN} = 0.01$ nM hr^{-1}, $n = 4$. The concentration scale is expressed, tentatively, in nM. Given that quantitative experimental data are still lacking, the above parameter values, which are in a physiological range, have been selected arbitrarily so as to yield a period close to 24 hr.

considered, the mean interval between two peaks of the complex is much larger than 24 hr. It is easy to reduce the parameter values of the model so as to bring this interval closer to 24 hr. We did not attempt to do this, however, because we do not want to stress any physiological implications of chaos for the *Drosophila* circadian system. Rather we wish to study the origin of chaotic oscillations in this model, which was constructed for periodic rather than chaotic behavior. Furthermore, if chaos arises in this model, we wish to know in what conditions and with what temporal characteristics it occurs as compared with the "basic" conditions in which the model generates truly periodic, circadian oscillations.

The strange attractor corresponding to the aperiodic oscillations of Fig. 3 is represented in Fig. 4 as a projection onto the three-variable space (M_P, M_T, C_N). The narrow funnel along which nearly all trajectories pass during a cycle is responsible for the small-amplitude peaks which follow the larger peaks in M_P and, to a

lesser extent, M_T (see Fig. 3). After exiting from this funnel the system generally undergoes a large excursion, giving rise to a large-amplitude peak in C_N. Sometimes, however, when the trajectory exits the funnel at its lower boundary (this happens after an excursion of extremely large amplitude), the system returns to the right part of the funnel without undergoing another large-amplitude excursion. Reinjection after passage through the funnel is responsible for the irregular oscillations associated with chaos.

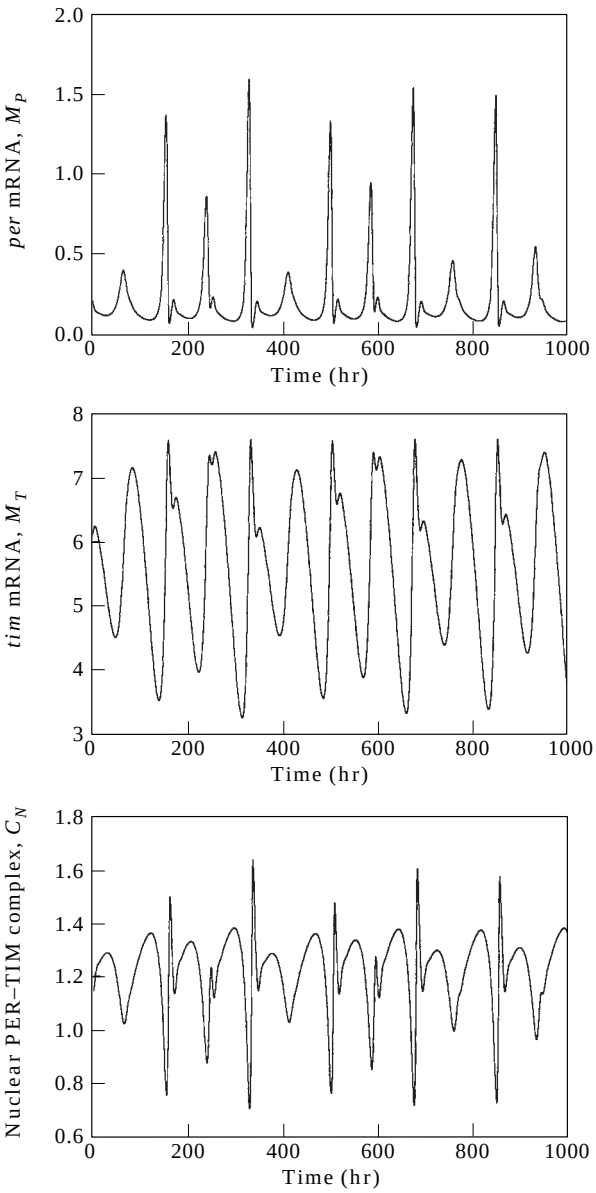

FIG. 3. Chaotic oscillations illustrated by the aperiodic variation in *per* mRNA (upper panel), *tim* mRNA (middle panel), and nuclear PER–TIM complex (bottom panel). The curves are obtained by numerical integration of eqns (1a)–(1j) for $v_{mT} = 0.28$ nM hr^{-1} and $v_{dT} = 4.8$ nM hr^{-1}; other parameter values are the same as in Fig. 2.

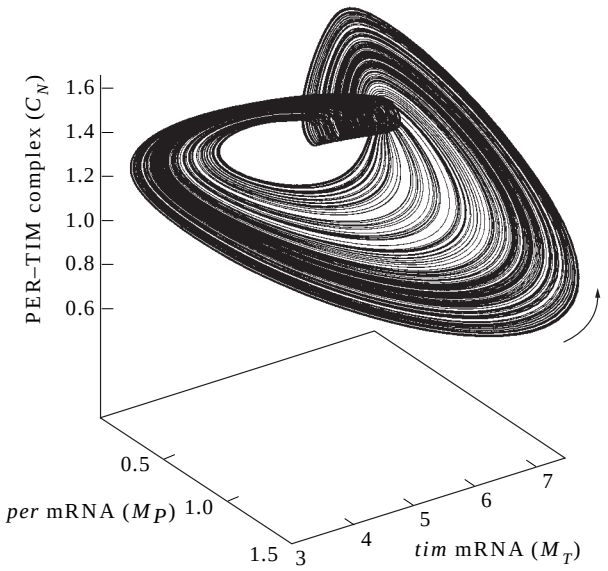

FIG. 4. Strange attractor corresponding to the chaotic oscillations shown in Fig. 3. The curve is obtained by projecting into the three-variable space (M_P, M_T, C_N) the trajectory followed by the 10-variable system governed by eqns (1a)–(1j).

The chaotic nature of the oscillations shown in Fig. 3 can be ascertained by means of Poincaré sections, as exemplified in Fig. 5 where the $(n + 1)$th maximum in the fully phosphorylated form of TIM (T_2) is plotted as a function of the n-th maximum in this variable. The continuous

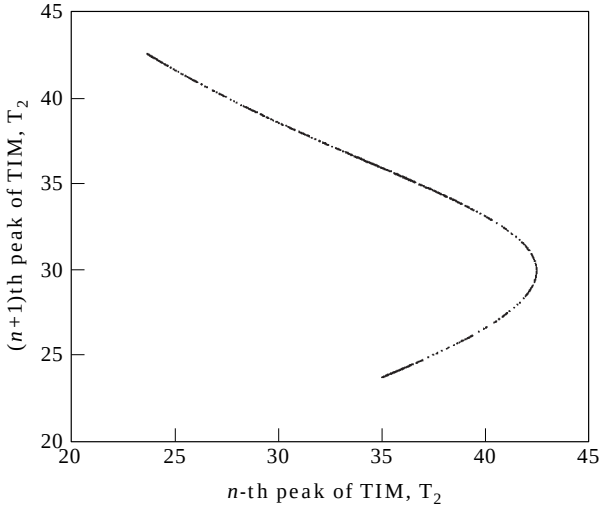

FIG. 5. Poincaré section showing the peak of the variable T_2 as a function of the preceding peak, in the case of Figs 3 and 4. The continuous, open appearance of the curve reflects the chaotic nature of the oscillations in Fig. 3.

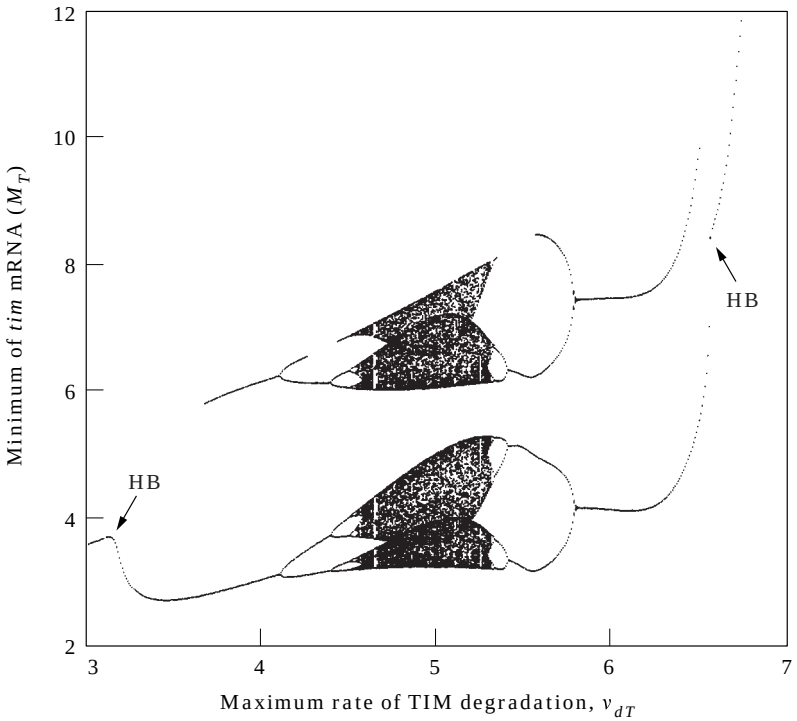

FIG. 6. Bifurcation diagram established as a function of the maximum rate of TIM degradation, v_{dT} (tentatively in nM hr^{-1}). Shown are the stable steady state and the minimum (or multiple minima) of *tim* mRNA (M_T) in the course of sustained oscillations. The points of Hopf bifurcation corresponding to the onset of limit cycle oscillations are denoted by HB. Parameter values are as in Fig. 3.

(but not closed) form of the curve thus obtained is a signature of the occurrence of chaotic behaviour.

A typical bifurcation diagram for the occurrence of chaos in this model is shown in Fig. 6. Plotted there is the minimum of variable M_T as a function of parameter v_{dT} which measures the rate of degradation of the TIM protein. The data have been obtained by numerical integration of eqns (1a)–(1j). At both the left and right extremities, when the steady state becomes unstable and oscillations appear at the Hopf bifurcation points marked HB, a single minimum per period is obtained; the system then operates in the region of simple periodic behavior. Increasing v_{dT} from a low initial value leads to the appearance of a second, higher minimum in M_T which is associated with a small loop that is the precursor of the funnel in Fig. 4. A sequence of period-doubling bifurcations occurs as v_{dT} increases, until chaos is reached. Entry into the chaotic domain upon decreasing v_{dT} from a large initial value again occurs through a sequence of period-doubling bifurcations. The two ramifying branches of minima in Fig. 6 are associated with the large-amplitude excursions and with the small-amplitude funnel that are visible in Figs 3 and 4. The separation between the two branches corresponds to the hole in the middle of the strange attractor (see Fig. 4). The parts which seem to be missing on some of the upper branches (for example around $v_{dT} = 3.5$ or 5.5) are due to the fact that the small loop after a large-amplitude peak in M_T is not fully developed and only corresponds to a shoulder but not to a true local minimum in M_T.

To characterize the sensitivity of chaotic dynamics, we have determined for each parameter of the model the range over which chaos is observed in a given set of conditions. To this end, as indicated in Table 1, each parameter was assigned its basal value (given in Fig. 2), except v_{mT} and v_{dT} which were given, respectively, the values 0.35 and 5.30 (in nM hr^{-1}) corresponding to a point located in the middle of the region of

TABLE 1

Parameter sensitivity for chaotic dynamics. Shown for each parameter are the basal values corresponding to a point located in the middle of the domain of chaos in Fig. 10, *as well as the lower* (*LT*) *and upper threshold* (*UT*) *values bounding the domain of chaos when other parameters are given their basal values. The last two columns give the range* (*expressed in % of the basal value*) *over which each parameter, varied one at a time below and above the basal value, produces chaos. The basal values are those indicated in Fig.* 2, *except for* ν_{mT} *and* ν_{dT} (*to indicate this, the values of these two parameters are listed in bold type*). *The data have been obtained by constructing bifurcation diagrams as a function of each parameter by numerical integration of eqns* (1*a*)–(1*j*). *Small windows of periodic behaviour are sometimes found within the domain of chaos indicated in the table*

Parameter	Basal value	Lower threshold (LT)	Upper threshold (UT)	Percentage variation between the LT and the basal value (%)	Percentage variation between the UT and the basal value (%)
v_{mP} (nM hr^{-1})	0.70	0.65	0.80	−7.0	+14.3
v_{mT} (nM hr^{-1})	**0.35**	0.28	0.39	−20.0	+11.3
v_{dP} (nM hr^{-1})	2.00	1.30	4.29	−35.0	+114.5
v_{dT} (nM hr^{-1})	**5.30**	4.80	6.10	−9.4	+15.1
v_{sP} (nM hr^{-1})	1.00	0.89	1.07	−11.0	+7.0
v_{sT} (nMhr^{-1})	1.00	0.92	1.31	−8.0	+31.0
$V_{1P} = V_{3P}$ (nM hr^{-1})	8.0	4.64	39.5	−42.0	+393.7
$V_{2P} = V_{4P}$ (nM hr^{-1})	1.0	0.51	2.69	−49.0	+169.0
$V_{1T} = V_{3T}$ (nM hr^{-1})	8.0	7.16	8.44	−10.5	+5.5
$V_{2T} = V_{4T}$ (nM hr^{-1})	1.0	0.42	1.87	−58.0	+87.0
k_1 (hr^{-1})	0.60	0.17	0.89	−71.7	+48.3
k_2 (hr^{-1})	0.20	0.14	0.43	−30.0	+115.0
k_3 (nM^{-1} hr^{-1})	1.20	0.35	1.9	−70.8	+58.3
k_4 (hr^{-1})	0.60	0.40	1.46	−33.3	+143.3
k_{sP} (hr^{-1})	0.90	0.43	1.31	−52.2	+45.6
k_{sT} (hr^{-1})	0.90	0.76	1.17	−15.6	+30.0
K_{IP} (nM)	1.0	0.91	1.03	−9.0	+3.0
K_{IT} (nM)	1.0	0.97	1.05	−3.0	+5.0

chaos in the diagram of Fig. 10. Then, each parameter was varied, one at a time, to determine percentage variation below and above its basal value, required to move out from the domain of chaotic oscillations.

The results, given in Table 1, indicate that autonomous chaos is a rather robust phenomenon in the model since the range of values producing aperiodic oscillations is larger (and often much larger) than $\pm 10\%$ for nearly all parameters, with the exception of the threshold constants for inhibition of *per* and *tim* expression for which the range of values associated with chaos is more reduced. The domain of values associated with chaos is also more reduced for the rates of phosphorylation of TIM ($V_{1T} = V_{3T}$) as compared with the rates of PER phosphorylation ($V_{1P} = V_{3P}$). Similarly, the range of the TIM degradation rate (v_{dT}) producing chaos is smaller than the corresponding range for the rate of PER degradation (v_{dP}).

4. Birhythmicity

For other parameter values, the system can also display the property of birhythmicity. As will be shown in the next section, two main regions of birhythmicity have been found in the v_{mT}–v_{dT} parameter plane. The occurrence of birhythmicity in these two regions is illustrated in the bifurcation diagrams established in Fig. 7 as a function of parameter v_{mT} for $v_{dT} = 2$ nM hr^{-1} (left column) and 3.8 nM hr^{-1} (right column), respectively. Shown from top to bottom in Fig. 7 are the minimum and maximum of the oscillations in *per* mRNA (M_P) and in *tim* mRNA (M_T), as well as the period of the oscillations. In each case birhythmicity

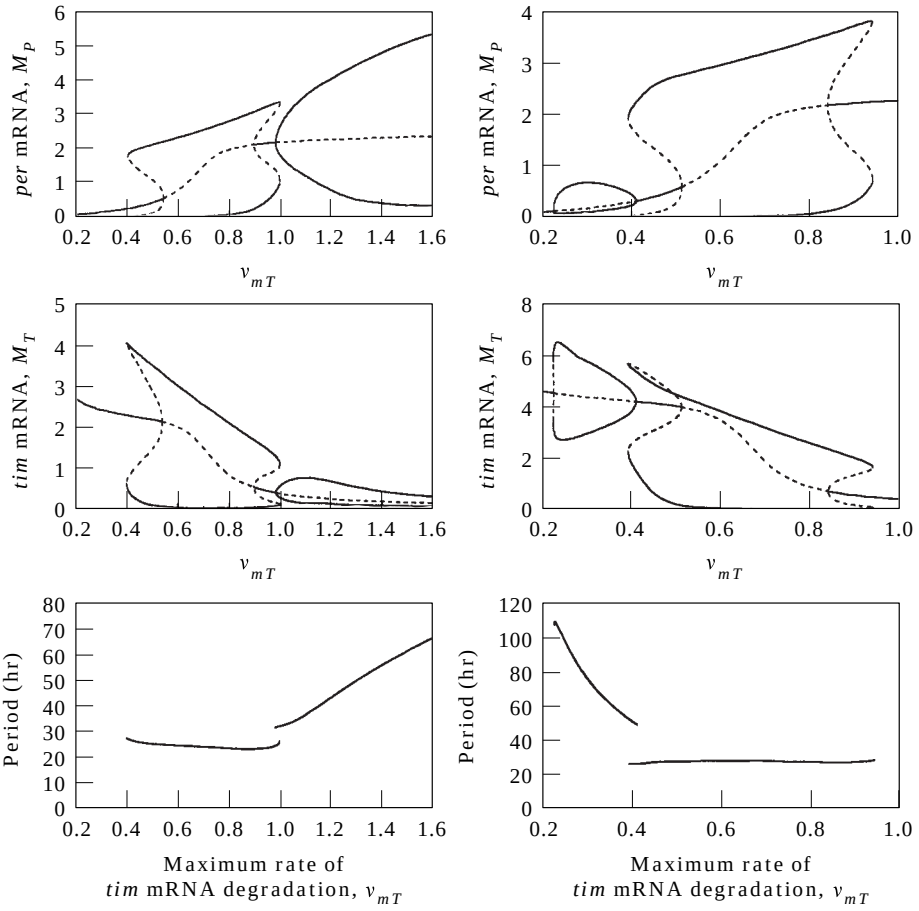

FIG. 7. Birhythmicity. The region of coexistence between two stable limit cycles is seen on the bifurcation diagrams established as a function of parameter v_{mT} (tentatively in nM hr^{-1}) for two distinct values of the maximum rate of TIM degradation corresponding to two distinct domains of birhythmicity in the v_{mT}–v_{dT} parameter plane (see Fig. 10): $v_{dT} = 2.0$ nM hr^{-1} (left column), and $v_{dT} = 3.8$ nM hr^{-1} (right column). The bifurcation diagrams show the stable steady state or the maximum and minimum of variables M_P (upper panels) and M_T (middle panels). The curves showing the variation of the period as a function of v_{mT} clearly indicate that two branches of sustained oscillations overlap over a small range of v_{mT} values for the two values of v_{dT} listed above. The curves are obtained by means of the program AUTO (Doedel, 1981); other parameter values are as in Fig. 2.

occurs when two domains of oscillations, separated by a domain of stable steady states, overlap because one of the limit cycles originates from a subcritical Hopf bifurcation. A similar situation was previously encountered in a model of two autocatalytic enzyme reactions coupled in series (Decroly & Goldbeter, 1982; Goldbeter, 1996).

The comparison of the bifurcation diagrams indicates that at the lower value of v_{dT} (left column), the domain of oscillations on the left (corresponding to low values of v_{mT}) is associated with such subcritical Hopf bifurcations. The right part of this domain then overlaps with the domain of oscillations on the right, seen at higher values of v_{mT}, so that birhythmicity occurs in a narrow region where two stable periodic solutions coexist. In contrast, at the higher value of v_{dT} (right column), the mirror situation is obtained since the subcritical Hopf bifurcations are now associated with the oscillatory domain found on the right at large values of v_{mT}.

The phase space orbits corresponding to the two cases of coexisting limit cycles examined in Fig. 7 are shown in Fig. 8 as projections of the trajectory followed by the 10-variable system onto the M_P–M_T plane. The time course of M_P, M_T, total PER and total TIM associated with the two types of oscillations in each of the two domains of birhythmicity is shown in Fig. 9. In each of the two cases of birhythmicity, the

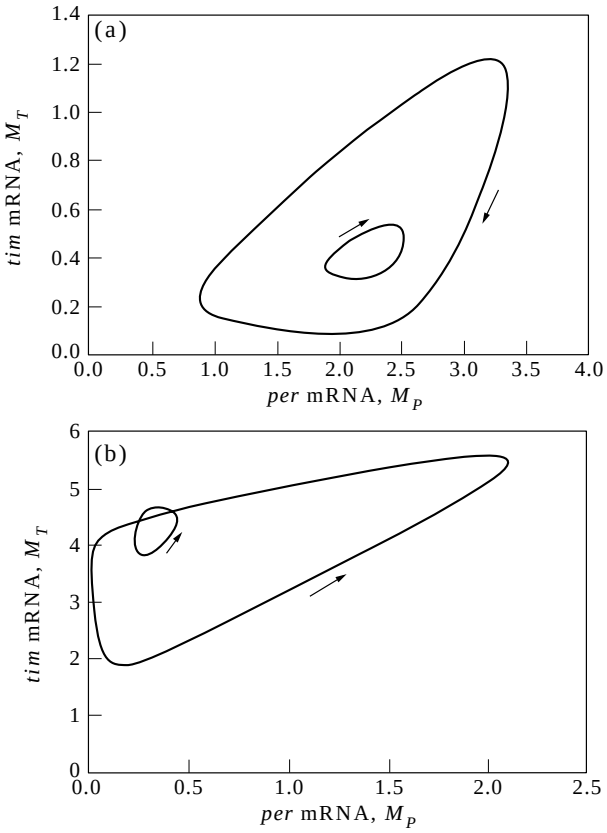

FIG. 8. Birhythmicity. The two coexisting limit cycles, obtained by numerical integration of eqns (1a)–(1j) are projected onto the M_P–M_T plane, in the two cases considered in Fig. 7: (a) $v_{dT} = 2.0$ nM hr^{-1}, $v_{mT} = 0.99$ nM hr^{-1}; (b) $v_{dT} = 3.8$ nM hr^{-1}, $v_{mT} = 0.4$ nM hr^{-1}. The arrows indicate the direction of movement along the periodic orbits.

amplitude of the two limit cycles is markedly different (see also Fig. 8). The period can also differ significantly for the two cycles, as clearly exemplified by the situation considered at the highest value of v_{dT} (see right column, bottom panel in Fig. 9). Interestingly, the smallest of the two limit cycles is also that which is associated with the longest period, even though the parameter values are the same for the two cycles. This illustrates the fact that, in contrast to commonly held views (see, e.g. Lakin-Thomas *et al*., 1991), the increase in size of a limit cycle is not necessarily accompanied by a rise in period of the associated oscillations.

5. Complex Dynamics in Parameter Space

To get insight into the relative importance of the various domains of complex oscillatory phenomena in parameter space, we have established a diagram showing the domains of different dynamic behaviour in the v_{mT}–v_{dT} parameter plane. The bottom part of this diagram (Fig. 10), which extends over two orders of magnitude of v_{mT} and four orders of magnitude of v_{dT}, shows the existence of a domain of stable steady states (SSS), as well as a small and a large domain of periodic oscillations (PO). For the small periodic domain on the left, we observe period-doubling bifurcations (PD) leading to chaos (C) (see the enlargement of this region of the parameter space in the upper, left panel). Both for the small and the large domains of periodic behavior, we find a region of hard excitation (HE) in which a stable steady state coexists with a stable limit cycle, as a result of the birth of the latter from a subcritical Hopf bifurcation (see also Fig. 7 where the role of this subcritical bifurcation in the occurrence of birhythmicity is illustrated). Birhythmicity (B) in Fig. 10 is found in two regions (see enlargements in the two upper panels) where a domain of periodic oscillations is adjacent to a domain of hard excitation. Hard excitation is also observed in a tiny, third region in the v_{mT}–v_{dT} parameter plane (see upper left panel).

Birhythmicity can also involve the coexistence between a stable limit cycle and a stable strange attractor. Such a coexistence, also observed in other models (Decroly & Goldbeter, 1982), was found in the present model (Fig. 11) for parameter values other than those considered in Fig. 10.

From the diagram of Fig. 10 we may conclude that periodic oscillations remain the most common mode of oscillatory behavior predicted by the model. This is satisfactory, since the model primarily aims at accounting for regular oscillations of circadian period in *Drosophila*. The diagram indicates, however, that complex oscillatory phenomena can also occur in this model in domains of progressively decreasing size for hard excitation, chaos, and birhythmicity.

6. Discussion

The present results on the occurrence of complex oscillatory phenomena in a realistic

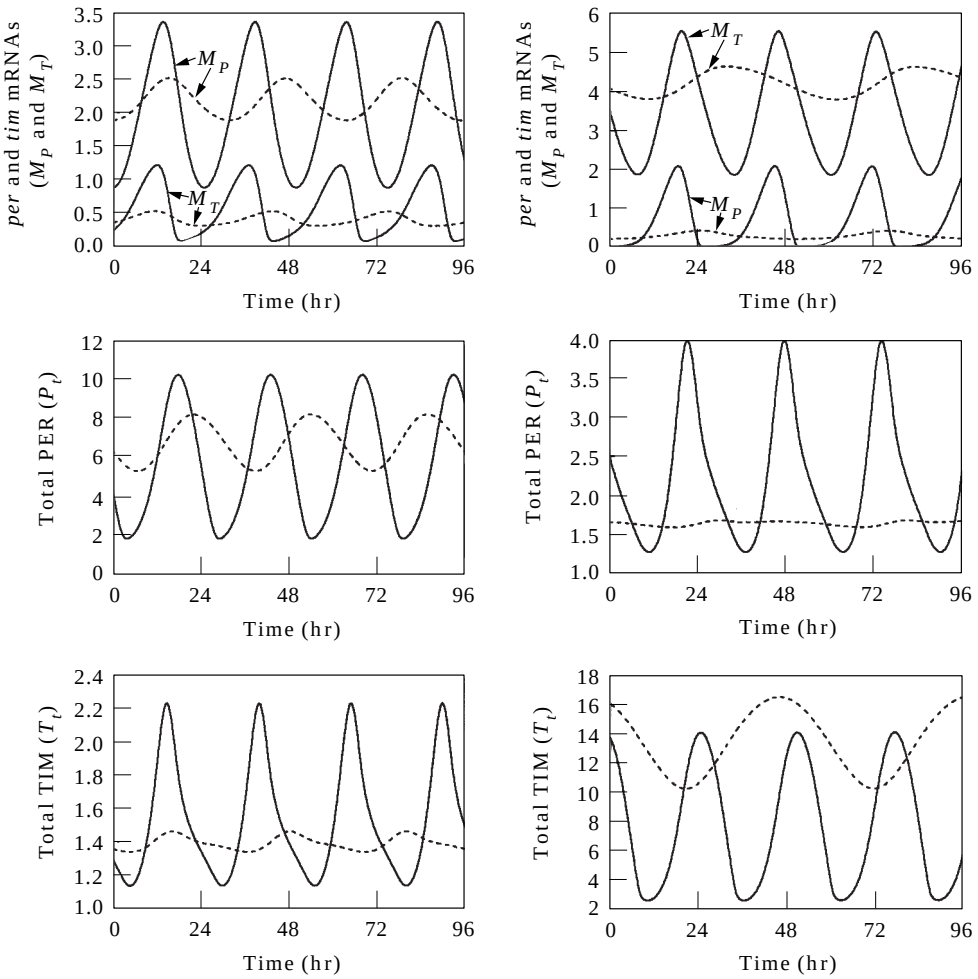

FIG. 9. The coexistence between two regimes of sustained oscillations corresponding to the large (——) and small (– – –) limit cycles shown in Fig. 8 is illustrated for $v_{dT} = 2.0$ nM hr^{-1} (left column) and $v_{dT} = 3.8$ nM hr^{-1} (right column) by the time variation of the *per* and *tim* mRNAs (upper panels) and of the total amounts of PER (middle panels) and TIM (lower panels) proteins.

model for circadian oscillations in *Drosophila* are of particular interest for understanding the conditions in which chaos and birhythmicity may arise in biological systems. The first evidence pointing to these phenomena in the present model was obtained by chance (the first indication of complex oscillatory phenomena observed in the numerical simulations was the finding of birhythmicity in the small domain shown in the upper right panel in Fig. 10).

Complex oscillatory phenomena, including chaos, may readily arise from the periodic forcing of an oscillatory system. Thus, chaos has been recently found in a circadian model forced by periodic LD cycles (Gonze *et al*., 1999). Here, in contrast, we focused on the case where chaos and birhythmicity occur in the model for circadian oscillations in *Drosophila* in constant environmental conditions, i.e. in constant darkness or constant light. Autonomous chaos and birhythmicity often occur as a result of the interplay between two instability-generating mechanisms coupled within the same system (Goldbeter, 1996). Thus the phenomena have been demonstrated in a three-variable model for two autocatalytic enzyme reactions coupled in series (Decroly & Goldbeter, 1982), and in a model for cyclic AMP signalling in *Dictyostelium* amoebae (Martiel & Goldbeter, 1985), in which two biochemical oscillators are coupled in parallel. The latter two oscillators share a common positive feedback loop, but differ by the process that limits this self-amplification. More recently chaos and birhythmicity have been

found in a skeleton model for the coupling through mutual inhibition of two biochemical oscillators controlling different phases of the cell cycle (Romond *et al*., 1999). The interaction between two oscillators, however, is not required for the generation of chaos. Thus the phenomenon may also result from the self-modulation by an oscillatory system of one of the parameters that control its evolution, as shown by the study of chaos in a model for intracellular Ca^{2+} signalling (Borghans *et al*., 1997; Houart *et al*., 1999).

Here, the situation responsible for the occurrence of complex oscillatory phenomena, including autonomous chaos, can also be related to the coupling in parallel of two endogenous oscillatory mechanisms. Indeed, the model of Fig. 1 involves a single feedback loop that relies on the negative control exerted by the nuclear PER–TIM complex on gene expression. The

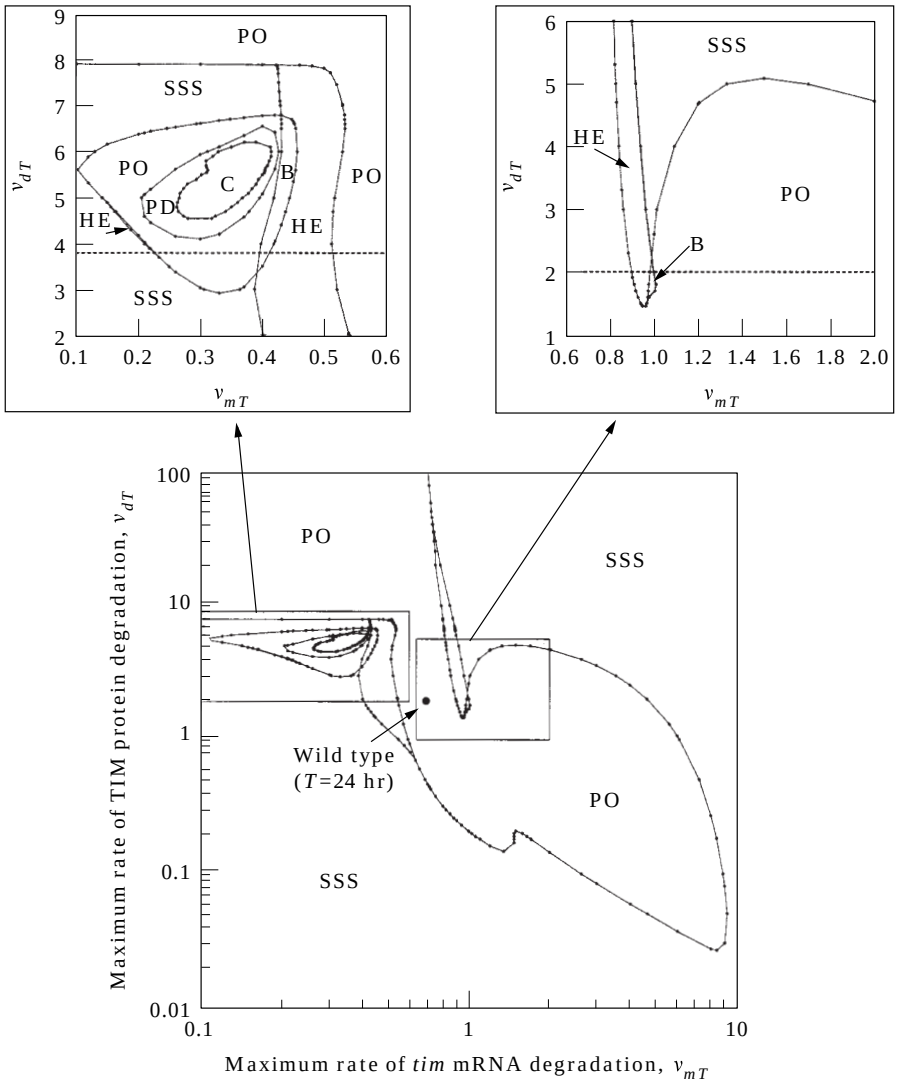

FIG. 10. Stability diagram established as a function of parameters v_{mT} and v_{dT}, showing the different modes of simple or complex oscillatory behavior in this parameter plane (see text). Shown are the regions of occurrence of a stable steady state (SSS), periodic oscillations (PO), period-doubling (PD), chaos (C), birhythmicity (B), and hard excitation (HE). (•) refers to the case that corresponds to the periodic circadian oscillations shown in Fig. 2. The stability diagram is established over several orders of magnitude of the two control parameters (lower panel) by means of the program AUTO (Doedel, 1981). The two boxed domains are enlarged in the upper panels. (– – –) in the latter panels refer to the two distinct values of v_{dT} used for the bifurcation diagrams established as a function of v_{mT} to illustrate birhythmicity in Fig. 7. Parameter values are as in Fig. 2.

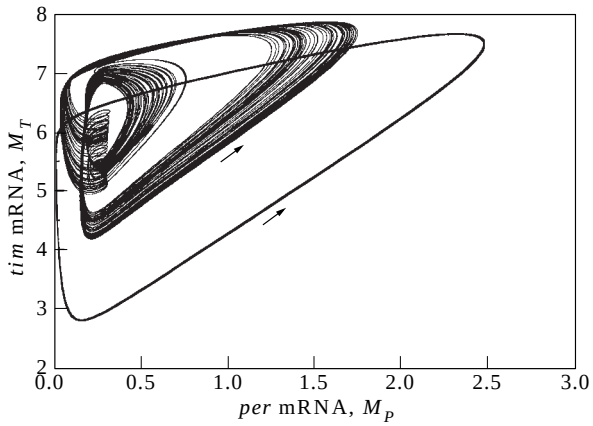

FIG. 11. Coexistence between a stable limit cycle and a stable chaotic attractor. The curves have been obtained, starting from different initial conditions, by integration of eqns (1a)–(1j) for $v_{dT} = 5.3$ nM hr^{-1}, $v_{mT} = 0.35$ nM hr^{-1}, $V_{1P} = V_{3P} = 4.69$ nM hr^{-1}. Other parameter values are as in Fig. 2.

Drosophila control system schematized in Fig. 1 nevertheless possesses two distinct branches, one involved in the synthesis of the TIM protein, and the other involved in that of PER. The two branches merge with the formation of the PER–TIM complex. Only simple periodic oscillations are found when this system is fully symmetrical, i.e. when the PER and TIM branches of the model are characterized by the same parameter values for all corresponding steps. If different values are considered, simple periodic oscillations remain the most common mode of oscillatory behavior in parameter space, as shown in Fig. 10 (see also Leloup & Goldbeter, 1998). Chaos may occur, however, when the two branches of the oscillatory system are out of "synchrony", which happens when they differ sufficiently by the value of important control parameters such as the rates of degradation of *tim* mRNA or of TIM protein with respect to those related to *per* mRNA or PER.

The asymmetry between the PER and the TIM branches is necessary but not sufficient to produce chaos. For the latter to occur, some antagonistic effects on one of the two proteins are apparently needed. Thus, in Fig. 10, chaos occurs in a region where small values of v_{mT} increase the concentration of the *tim* mRNA, and therefore the concentration of the TIM protein, while high values of v_{dT} decrease the latter concentration. However, we did not observe chaos at high values of v_{mT} and low values of v_{dT} (see Fig. 10). Therefore, besides noticing the need for asymmetries in the two branches of the genetic control system, it is difficult to propose at this stage a more precise explanation for the occurrence of chaos in this model if only because periodic oscillations always remain the most common type of oscillatory behavior, even in the case of asymmetric conditions.

It is tempting to speculate on the biological significance of the results in regard to circadian rhythm generation. We are reluctant to indulge in such speculations and therefore did not make any attempt to rescale the parameter values (which we previously used to account for periodic oscillations of approximately 24 hr period) so as to obtain a mean value close to 24 hr for the interval between peaks of chaotic oscillations. A first caveat, indeed, pertains to the relative smallness of the domains in parameter space in which birhythmicity and chaos occur. The size of the domain of complex oscillations depends, of course, on the values of the other parameters of the model. Our conclusions on the relative smallness of the domains of chaos and birhythmicity as compared with the domains of periodic behavior are based on the diagram of Fig. 10 but also on numerical simulations performed with other parameter values.

A second caveat, with regard to chaos, is that if arrhythmic mutants of the circadian clock are known in *Drosophila* (Konopka & Benzer, 1971; Sehgal *et al*., 1994; Vosshall *et al*., 1994), this behavior seems to result from a deletion of a clock gene such as *per* or *tim*, or from a non-functional, truncated PER or TIM protein (Yu *et al*., 1987; Sehgal *et al*., 1994; Vosshall *et al*., 1994), rather than from a change in a control parameter that would lead to the transition from periodic to chaotic oscillations, as described in the present study.

If arrhythmic behavior were due to the chaotic dynamics of the PER–TIM control system, the question would arise as to the effect of entrainment by a light–dark cycle on such an aperiodic behavior. Numerical simulations in which the light-controlled TIM degradation rate v_{dT} varies in a square-wave manner show that chaos can transform into periodic behavior if the

amplitude of the periodic variation in v_{dT} is sufficiently large. On the other hand, the fact that chaos is characterized by the sensitivity to initial conditions might result in a marked reduction of the oscillations in PER and TIM at the level of populations of cells or organisms. Indeed, if the individual oscillators were not strongly coupled, the lability of their phases in the chaotic mode could result in the overall quenching of the oscillations in the average protein levels.

Finally, birhythmicity might be related to the phenomenon of rhythm splitting (Pittendrigh, 1960) which refers to the separation of two rhythms, which initially have the same period, into two rhythms of markedly different periods in a system placed in constant environmental conditions. Such a splitting could, however, be due to the operation of two different oscillators which progressively lose their synchrony.

Regardless of the relatively small size of the domains in which they occur in parameter space and of their possible lack of physiological significance in regard to circadian rhythmicity, the fact that chaos and birhythmicity are found in the present realistic model suggests that such complex oscillatory phenomena should not be too uncommon in biological systems exhibiting simple periodic behaviour, given that these systems are often controlled by multiple mechanisms of cellular regulation.

This work was supported by the programme "Actions de Recherche Concertée" (ARC 94-99/180) launched by the Division of Scientific Research, Ministry of Science and Education, French Community of Belgium. J.-C. Leloup holds a research fellowship from F.R.I.A.

REFERENCES

Allada, R., White, N. E., So, W. V., Hall, J. C., & Rosbash, M. (1998). A mutant *Drosophila* homolog of mammalian *clock* disrupts circadian rhythms and transcription of *period* and *timeless*. *Cell* **93,** 791–804.

Baylies, M. K., Weiner, L., Vosshall, L. B., Saez, L. & Young, M. W. (1993). Genetic, molecular, and cellular studies of the *per* locus and its products in *Drosophila melanogaster*. In: *Molecular Genetics of Biological Rhythms* (Young, M. W., eds) pp. 123–153. New York: M. Dekker.

Borghans, J. A. M., Dupont, G. & Goldbeter, A. (1997). Complex intracellular calcium oscillations. A theoretical exploration of possible mechanisms. *Biophys. Chem.* **66,** 25–41.

Crosthwaite, S. K., Dunlap, J. C. & Loros, J. L. (1997). *Neurospora wc*-1 and *wc*-2: transcription, photoresponses, and the origins of circadian rhythmicity. *Science* **276,** 763–769.

Darlington, T. K., Wager-Smith, K., Ceriani, M. F., Staknis, D., Gekakis, N., Steeves, T. D. L., Weitz, C. J., Takahashi, J. S. & Kay, S. A. (1998). Closing the circadian loop: CLOCK-induced transcription of its own inhibitors *per* and *tim*. *Science* **280,** 1599–1603.

Decroly, O. & Goldbeter, A. (1982). Birhythmicity, chaos, and other patterns of temporal self-organization in a multiply regulated biochemical system. *Proc. Nat. Acad. Sci. U.S.A.* **79,** 6917–6921.

Doedel, E. J. (1981). AUTO: a program for the automatic bifurcation analysis of autonomous systems. *Congr. Num.* **30,** 265–284.

Dunlap, J. C. (1996). Genetics and molecular analysis of circadian rhythms. *Annu. Rev. Genet.* **30,** 579–601.

Edery, I., Zwiebel, L. J., Dembinska, M. E. & Rosbash, M. (1994). Temporal phosphorylation of the *Drosophila period* protein. *Proc. Nat. Acad. Sci. U.S.A.* **91,** 2260–2264.

Goldbeter, A. (1995). A model for circadian oscillations in the *Drosophila period* (PER) protein. *Proc. R. Soc. Lond. B* **261,** 319–324.

Goldbeter, A. (1996). *Biochemical Oscillations and Cellular Rhythms*: *The Molecular Bases of Periodic and Chaotic Behaviour*. Cambridge: Cambridge University Press.

Gonze, D., Leloup, J.-C. & Goldbeter, A. (1999). Theoretical models for circadian oscillations in *Neurospora* and *Drosophila*. *C. R. Acad. Sci.* (*Paris*) *III* (in press).

Goodwin, B. C. (1965). Oscillatory behavior in enzymatic control processes. *Adv. Enzyme Regul.* **3,** 425–438.

Hall, J. C. (1995). Tripping along the trail to the molecular mechanisms of biological clocks. *Trends Neurosci.* **18,** 230–240.

Hall, J. C. & Rosbash, M. (1987). Genes and biological rhythms. *Trends Genet.* **3,** 185–191.

Houart, G., Dupont, G. & Goldbeter, A. (1999). Bursting, chaos and birhythmicity originating from self-modulation of the inositol 1,4,5-triphosphate signal in a model for intracellular Ca^{2+} oscillations. *Bull. Math. Biol.* **61,** 507–530.

Hunter-Ensor, M., Ousley, A. & Sehgal, A. (1996). Regulation of the *Drosophila* protein Timeless suggests a mechanism for resetting the circadian clock by light. *Cell* **84,** 677–685.

Koike, N., Hida, A., Numano, R., Hirose, M., Sakaki, Y. & Tei, H. (1998). Identification of the mammalian homologues of the *Drosophila timeless* gene, *Timeless*1. *FEBS Lett.* **441,** 427–431.

Konopka, R. J. & Benzer, S. (1971). Clock mutants of *Drosophila melanogaster*. *Proc. Nat. Acad. Sci. U.S.A.* **68,** 2112–2116.

Kloss, B., Price, J. L., Saez, L., Blau, J., Rothenfluh, A., Wesley, C. S. & Young, M. W. (1998). The *Drosophila* clock gene *double-time* encodes a protein closely related to human casein kinase Iε. *Cell* **94,** 97–107.

Lakin-Thomas, P. L., Brody, S. & Cote, G. C. (1991). Amplitude model for the effects of mutations and temperature on period and phase resetting of the *Neurospora* circadian oscillator. *J. Biol. Rhythms* **6,** 281–297.

Lee, C., Parikh, V., Itsukaichi, T., Bae, K. & Edery, I. (1996). Resetting the *Drosophila* clock by photic

regulation of PER and a PER–TIM complex. *Science* **271,** 1740–1744.

Leloup, J.-C. & Goldbeter, A. (1998). A model for circadian rhythms in *Drosophila* incorporating the formation of a complex between the PER and TIM proteins. *J. Biol. Rhythms* **13,** 70–87.

Myers, M. P., Wager-Smith, K., Rothenfluh-Hilfiker, A. & Young, M. W. (1996). Light-induced degradation of TIMELESS and entrainment of the *Drosophila* circadian clock. *Science* **271,** 1736–1740.

Pittendrigh, C. S. (1960). Circadian rhythms and the circadian organization of living systems. *Cold Spring Harb. Symp. Quant. Biol.* **25,** 159–182.

Price, J. L., Blau, J., Rothenfluh, A., Abodeely, M., Kloss, B. & Young, M. W. (1998). *Double-time* is a new *Drosophila* clock gene that regulates PERIOD protein accumulation. *Cell* **94,** 83–95.

Romond, P.-C., Rustici, M., Gonze, D. & Goldbeter, A. (1999). Alternating oscillations and chaos in a model of two coupled biochemical oscillators driving successive phases of the cell cycle. *Ann. N. Y. Acad. Sci.* (in press).

Rosbash, M. (1995). Molecular control of circadian rhythms. *Curr. Opin. Genet.* **5,** 662–668.

Ruoff, P., Mohsenzadeh, S. & Rensing, L. (1996). Circadian rhythms and protein turnover: the effect of temperature on the period lengths of clock mutants simulated by the Goodwin oscillator. *Naturwissenschaften* **83,** 514–517.

Rutila, J. E., Suri, V., Le, M., So, W. V., Rosbash, M. & Hall, J. C. (1998). CYCLE is a second bHLH-PAS clock protein essential for circadian rhythmicity and transcription of *Drosophila period* and *timeless*. *Cell* **93,** 805–814.

Sehgal, A., Price, J. L., Man, B. & Young, M. W. (1994). Loss of circadian behavioral rhythms and *per* RNA oscillations in the *Drosophila* mutant *timeless*. *Science* **263,** 1603–1606.

Shearman, L. P., Zylka, M. J., Weaver, D. R., Kolakowski, L. F. Jr. & Reppert, S. M. (1997). Two period homologs: circadian expression and photic regulation in the suprachiasmatic nuclei. *Neuron* **19,** 1261–1269.

Tei, H., Okamura, H., Shigeyoshi, Y., Fukuhara, C., Ozawa, R., Hirose, M. & Sakaki, Y. (1997). Circadian oscillation of a mammalian homologue of the *Drosophila period* gene. *Nature* **389,** 512–516.

Vosshall, L. B., Price, J. L., Sehgal, A., Saez, L. & Young, M. W. (1994). Block in nuclear localization of *period* protein by a second clock mutation, *timeless*. *Science* **263,** 1606–1609.

Yu, Q., Jacquier, A. C., Citri, Y., Hamblen, M., Hall, J. C. & Rosbash, M. (1987). Molecular mapping of point mutations in the *period* gene that stop or speed up biological clocks in *Drosophila melanogaster*. *Proc. Nat. Acad. Sci. U.S.A.* **84,** 784–788.

Zeng, H., Qian, Z., Myers, M. P. & Rosbash, M. (1996). A light-entrainment mechanism for the *Drosophila* circadian clock. *Nature* **380,** 129–135.

Zylka, M. J., Shearman, L. P., Levine, J. D., Jin, X., Weaver, D. R. & Reppert, S. M. (1998). Molecular analysis of mammalian *timeless*. *Neuron* **21,** 1115–1122.